Electronic and lattice structures in $SmFeAsO_{1-x}F_x$ probed by x-ray absorption spectroscopy

C. J. Zhang,[1] H. Oyanagi,[1,*] Z. H. Sun,[1] Y. Kamihara,[2] and H. Hosono[3]
[1]*National Institute of Advanced Industrial Science and Technology, 1-1-1 Umezono, Tsukuba 305-8568, Japan*
[2]*JST, TRiP, in Materials and Structures Laboratory, Tokyo Institute of Technology, 4259 Nagatsuta, Midori-ku, Yokohama 226-8503, Japan*
[3]*Materials and Structures Laboratory, Tokyo Institute of Technology, Mail Box R3-1, 4259 Nagatsuta, Midori-ku, Yokohama 226-8503, Japan*
(Received 31 August 2009; revised manuscript received 13 January 2010; published 17 March 2010)

Local lattice and electronic structures in the Fe-As layer of $SmFeAsO_{1-x}F_x$ superconductors were studied by x-ray absorption spectroscopy, the Fe *K*-edge and the As *K*-edge extended x-ray absorption fine-structure, and x-ray absorption near-edge-structure experiments, respectively. Temperature-dependent local lattice distortions were observed in the Fe-As bond mean-square relative displacement of the superconducting samples. A strong coupling of the carrier-induced local lattice distortion (polaron) to the superconducting transition temperature in the oxypnictide superconductors is indicated. The near-edge spectra showed systematic temperature-dependent energy shifts, which indicate an intralayer electron redistribution from Fe *d* states to As *p* states due to orbital-selective band filling at low temperatures.

DOI: 10.1103/PhysRevB.81.094516 PACS number(s): 74.70.−b, 61.05.cj, 71.20.−b, 74.81.−g

I. INTRODUCTION

In cuprate superconductors, the parent compounds are antiferromagnetic Mott insulators.[1] A small amount of carriers doped to this Mott insulating state drives a metal-insulator transition, and results in a superconducting transition. In contrast, in oxypnictide systems *RE*FeAsO (rare-earth element, *RE*), high-temperature superconductivity (HTSC) derives from either electron or hole doping of the semimetallic parent compounds[2–5] with hole and electron pockets around the Γ point and M point, respectively. Information on the local structure of oxypnictides is essential to understand the doping-induced electron states, particularly, complex band filling and disorder around dopant impurities.

Since the discovery of HTSC in $LaFeAsO_{1-x}F_x$, a number of theoretical calculations have been made regarding the role of electron correlations in *RE*FeAsO compounds.[6–9] Two distinct theoretical viewpoints, distinguished by the underlying band structure, have been put forward: a strong correlation approach which is close to the Mott transition criterion,[6,7] and a weak correlation approach which emphasizes an itinerant ground state.[8,9] These band calculations predicted a weak electron-phonon coupling constant which cannot explain the critical temperature ruling out phonon-mediated mechanism (BCS model). However, multiband nature of FeAs systems suggests proximity with multiband multigap superconductor MgB_2 where phonon-mediated superconductivity with interband interactions gives moderately high critical temperature.[10] Local lattice (distortion) in general is closely related to band splitting while in strongly correlated systems such as cuprates, pseudogap phase is attributed to polaron (localizing-doped carriers). Present work aims at investigating temperature-dependent local lattice distortion in SmFeAsO(F) systems to describe its role in microscopic pairing mechanism.

X-ray absorption spectroscopy (XAS) is a powerful experimental tool as a probe of instantaneous local (electronic and lattice) structures. Using O *K*-edge and Fe *L*-edge XAS measurements, Kroll *et al.* observed an energy shift in the threshold of core electron excitation as a result of carrier doping that varied the chemical potential, and emphasized the importance of band effects in $LaFeAsO_{1-x}F_x$ compounds.[11] Based on the Fe *K*-edge XAS measurement, Ignatov *et al.* also found a chemical shift to lower energy with F doping in $LaFeAsO_{1-x}F_x$ while no chemical shift was observed in the As *K*-edge XAS.[12] Those studies clearly showed that the effective number of electrons at the specific site change by doping indicating effective electrons are accommodated at Fe and As sites in the FeAs layer consistent with doping picture.

However, there has been no systematic study focusing on the doping and temperature evolution of the electronic structure and its relationship to superconductivity. In this work, we examined the local electronic structure of $SmFeAsO_{1-x}F_x$ compounds, using As *K*-edge and Fe *K*-edge x-ray absorption near-edge structure (XANES), and the local lattice structure using As *K*-edge extended x-ray absorption fine-structure (EXAFS) measurements. The combined experimental results indicate carrier-induced local lattice distortions in the Fe-As mean-square relative displacement (MSRD) and a strong temperature-dependent redistribution of charge (a charge transfer from Fe to As sites). The results suggest that polaron formation and evolution of coherence with decreasing temperature are closely related to the transport properties (critical temperature of superconductivity).

II. EXPERIMENT

Polycrystalline samples $SmFeAsO_{1-x}F_x$ ($x=0, 0.045, 0.069$) were prepared by solid-state synthesis.[2] The onset T_c (T_c) values were 14.8 (13) K and 50.8 (47) K for $x=0.045$ and $x=0.069$, respectively. As the doping dependence of the transport properties was quite sharp, it was essential to use samples with accurately determined compositions.[13] All XANES and EXAFS measurements were performed in a fluorescence mode at beamline BL13B

of the Photon Factory, Tsukuba, Japan. Fine powder samples embedded in an amorphous carbon film were mounted on an aluminum holder and attached to a closed-cycle helium refrigerator. The energy resolutions at the Fe *K* edge (7.11 keV) and As *K* edge (11.86 keV) were about 1 eV and 2 eV, respectively, using a double crystal Si(111) monochromator and vertically limited x-ray beam. For energy control and monitoring, high-precision angle encoder was used ensuring sequential near-edge measurement with energy uncertainty less than $0.5\times10^{-3\circ}$ or 0.04 meV at the Cu *K* edge (8.98 keV). The Fe *K*-edge and As *K*-edge data were sequentially recorded separately on slow heating. The helium cryostat mounted on a high-precision goniometer (Huber 420) was rotated to optimize the incidence angle.

A state-of-the-art Ge pixel array detector (PAD) with 100 segments was used in order to gain high throughput measurement of fluorescence yield. Systematic and nonsystematic noise was minimized by recording fluorescence signal of 4×10^6–5×10^6 photons/data after six runs of repeated scans. A detailed description of the PAD was reported elsewhere.[14] Most influential noise source is systematic origin caused by Laue diffractions and standing-wave excitations which are minimized by use of PAD. Monitoring output of segmented detector channels allows to measure EXAFS oscillations to high-*k* region, detecting small changes in mean-square relative displacement reflected in EXAFS magnitude change. Although real-space resolution that gives a separated Fourier-transform (FT) peak is approximately 0.1 Å for *k* range of 16 $Å^{-1}$, a separation down to 0.01 Å is detected by beat and analyzed by distortion model.[15,19]

III. RESULTS AND DISCUSSION

In order to investigate the local lattice anomaly in the Fe-As bond, we performed As *K*-edge EXAFS measurements on a series of $SmFeAsO_{1-x}F_x$ samples from 300 to 5 K. The As *K*-edge EXAFS oscillations of the undoped sample measured at 300 and 20 K are shown in Fig. 1(a). The enhanced magnitude of EXAFS oscillations at low temperature was due to a decrease in thermally induced vibration. The magnitudes of the Fourier transforms of the As *K*-edge EXAFS (multiplied by k^2) for the undoped sample at 300 and 20 K are shown in Fig. 1(b). The experimental EXAFS, $\chi(k)$, was analyzed by use of the IFFFIT analysis package.[16] An FEFF6 (Ref. 17) theoretical calculation of the EXAFS curve was performed for the crystallographic structure,[18] and adjustable structural parameters were added to the theory to account for possible deviations of the local structure from the average structure. The data were theoretically fitted in both *R* space and *k* space, and the uncertainties were determined from a reduced χ^2 using standard techniques of error analysis. In the fitted data, the coordination numbers were set to values dictated by the average structure. For the As-Fe correlation, the data were fitted over the $1.45<R<2.55$ Å region. Figure 1(c) shows temperature dependence of the intensity of the Fourier-transform magnitude curve for the nearest As-Fe correlation in $SmFeAsO_{1-x}F_x$ ($x=0.069$) sample. One can find a significant deviation from a smooth variation starting at around 60 K and a sharp

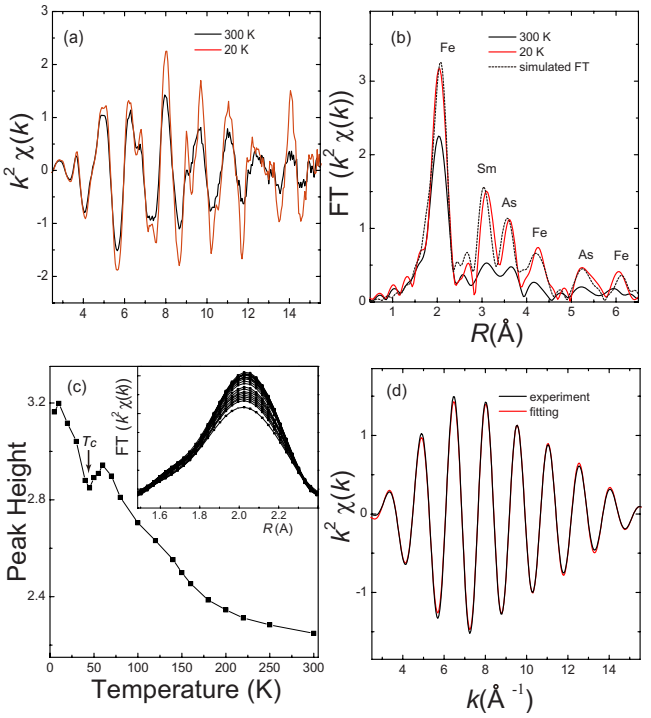

FIG. 1. (Color online) (a) Representative examples of As *K*-edge EXAFS oscillations recorded at 300 K (black, lower magnitude) and 20 K (red, higher magnitude). (b) Magnitudes of the Fourier transforms of the As *K*-edge EXAFS (multiplied by k^2) for the undoped sample. Dotted curve represents the theoretically simulated Fourier-transform magnitude of As *K*-edge EXAFS for 20 K data. (c) Temperature dependence of Fourier-transform peak intensity for the nearest-neighbor As-Fe correlation. Inset shows FT magnitudes measured at various temperatures. (d) Experimental first-shell As-Fe contribution to the As *K*-edge EXAFS oscillation at 300 K (black), and its comparison to the fitted theoretical curve based on a single-scattering formula and theoretical phase-shift functions (red).

change at the critical temperature of superconductivity (47 K). Typical results from fitted data for the first-shell As-Fe bond are shown in both *k* space [Fig. 1(d)]. Both fits gave identical results for the As-Fe bond distances summarized in Table I and the As-Fe bond MSRDs.

The temperature dependences of MSRD for the As-Fe bond ($\sigma^2_{\text{As-Fe}}$) in $SmFeAsO_{1-x}F_x$ ($x=0,0.045,0.069$) samples are compared with the results for $LaFeAsO_{1-x}F_x$ ($x=0,0.07$) in Fig. 2(a). For undoped SmFeAsO, $\sigma^2_{\text{As-Fe}}$ smoothly decreased with decreasing temperature, consistent with a noncorrelated Debye model indicating absence of lattice anomaly. In the F-doped samples, in contrast, an abrupt upturn of $\sigma^2_{\text{As-Fe}}$ was observed below about 60 K, followed by a sharp drop near the critical temperature of superconducting transition. This temperature-dependent unusual behavior of MSRD was similar to the local lattice anomaly observed in cuprates[15,19] and $LaFeAsO_{2-x}F_x$.[20] The results indicate the carrier-induced local lattice distortion (polaron formation) in $FeAs_4$ tetrahedra in *RE*FeAs (*RE*=La,Sm). The Fe-As bond length in the SmFeAsO system varied smoothly as temperature was lowered, suggesting no structural anomalies, in contrast to $LaFeAsO_{2-x}F_x$, which showed

TABLE I. A comparison of structure data of undoped SmFeAsO sample between the fitting results in k space and the fitting results in R space. In the fitting, the coordination number was set to 4 and the amplitude reduction factor S_0^2 was set to 0.72.

Temperature (K)	$R_{\text{As-Fe}}$ (Å)	MSRD (Å^2)	$R_{\text{As-Fe}}$ (Å)	MSRD (Å^2)
10	2.38651 (0.00315)	0.00148 (0.000186)	2.38644 (0.00353)	0.00151 (0.000187)
50	2.38743 (0.00361)	0.00151 (0.000181)	2.38706 (0.00333)	0.00150 (0.000172)
100	2.38793 (0.00383)	0.00173 (0.000221)	2.38791 (0.0038)	0.00172 (0.000201)
300	2.38989 (0.0046)	0.00339 (0.000256)	2.39011 (0.00449)	0.00345 (0.000239)

significant temperature-independent component (structural disorder) related to a magnetic phase transition.[21]

The temperature dependence of electrical resistivity and $\sigma^2_{\text{As-Fe}}$ for $SmFeAsO_{1-x}F_x$ together with those for $LaFeAsO_{1-x}F_x$ powder samples are plotted in Figs. 2(b) and 2(c), respectively, in an expanded scale. Note the nearly constant large $\sigma^2_{\text{As-Fe}}$ for the undoped LaFeAsO system in this range.[20] In contrast, SmFeAsO systems were characterized by a negligible amount of static (structural) disorder, which

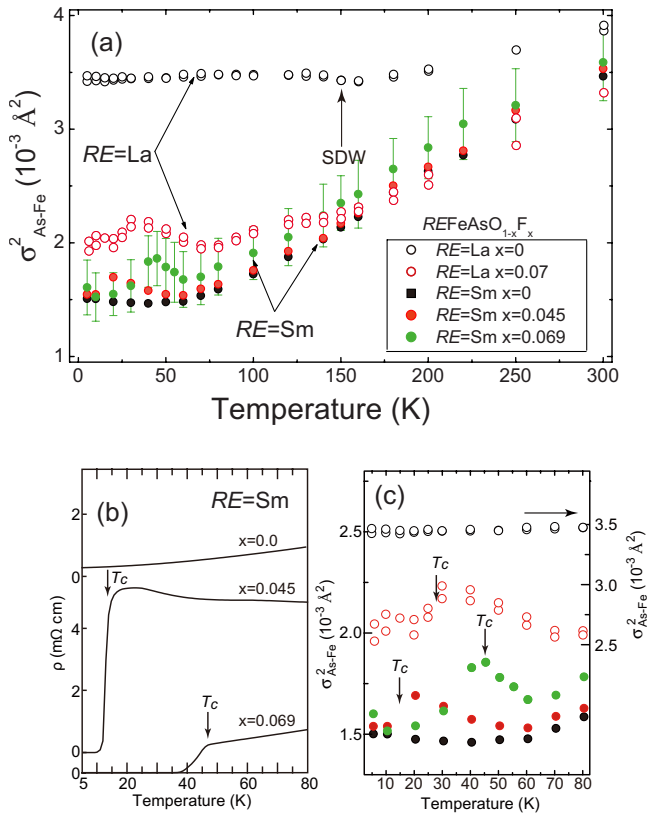

FIG. 2. (Color online) (a) Temperature dependence of As-Fe bond MSRD ($\sigma^2_{\text{As-Fe}}$) for $SmFeAsO_{1-x}F_x$ (x=0,0.045,0.069) samples compared with those for $LaFeAsO_{1-x}F_x$ (x=0,0.07) taken from Ref. 18. The arrow indicates the magnetic phase-transition temperature. (b) Temperature dependence of electrical resistivity of $SmFeAsO_{1-x}F_x$ (x=0,0.045,0.069). (c) Expanded temperature scale plots of (a), which indicates that the common upturn behavior below a characteristic temperature T^* followed by a sharp drop of MSRD at the onset of superconducting transition indicated by arrows.

may be a part of the reason for their higher T_c in SmFeAsO system. In both systems, undoped samples show no lattice anomalies while all superconducting, SmFeAsO(F) and LaFeAsO(F) samples showed an anomalous upturn of $\sigma^2_{\text{As-Fe}}$ below 60–70 K followed by a sharp drop at T_c. The former is a signature of local lattice distortion, i.e., a slowdown of polaron dynamics that causes the bond-length splitting observable with a fast time scale (10^{-13} s) local probe (EXAFS).[15,19] In contrast, the MSRD drop at T_c relates to fast polaron dynamics[22] which showed a remarkable correlation with the critical temperature of superconductivity.[23]

In the Fe-As system, we find precise correlation with the superconducting coherence probed by the local lattice and T_c. The superconducting transition temperature width values, ΔT_c, for the $SmFeAsO_{1-x}F_x$ samples were 10.3 K (x=0.069) and 4.3 K (x=0.045). Reflecting broader transition width, the former sample showed a broader drop in $\sigma^2_{\text{As-Fe}}$ at T_c, in contrast to LaFeAsOF and SmFeAsOF (x =0.045) as shown in Fig. 2(b). This indicates that the local instantaneous lattice reflecting polaron dynamics, correlates with the transport properties over a wide range in temperature (13–47 K). A similar correlation between atomic displacement and resistivity was also observed in cuprates, such as $La_{1.85}Sr_{0.15}CuO_4$.[15,19,21] The lattice distortion observed as anomalous temperature dependence of MSRD is described by a two-site distribution and interpreted as an inhomogeneous lattice with polarons with a slow dynamics (phonon softening).[22,24] For $La_{1.85}Sr_{0.15}CuO_4$, the nature of displacement was traced to the two possible *in-plane* lattice distortion modes, i.e., Q_2-type Jahn-Teller (JT) mode[24] or pseudo-JT (breezing) mode.[25] We note that a slowed down distortion giving rise to elongation and shrinking of the Fe-As bond would significantly affect the splitting of the two d_{3z^2-1} bands and density of states near the Fermi level E_F,[26] thereby influencing the magnetic instability and pseudogap opening. Although in FeAs systems, the calculated electron-phonon coupling constant is too weak to describe the T_c by several factors, it can be strongly enhanced by interband interaction in multiband superconductors such as MgB_2. Indeed, the electronic structure of FeAs systems resembles that of MgB_2 with respect to multiband nature and as local distortions influence band splitting and thereby magnetic instability caused by a large density of state at E_F. It could be this enhancement that enhances lattice-mediated superconductivity which needs systematic studies of temperature-dependent electronic and local structures.

Typical As K-edge XANES spectra taken at different temperatures for the F-doped sample, $SmFeAsO_{0.931}F_{0.069}$, are

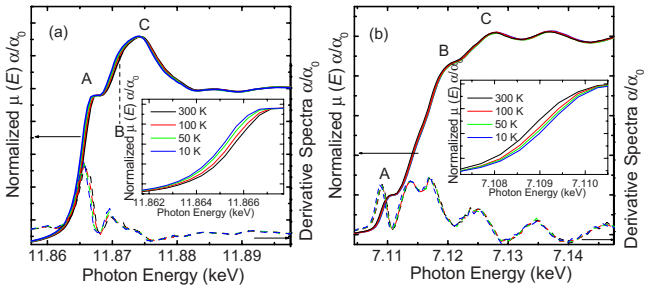

FIG. 3. (Color online) (a) A typical As *K*-edge XANES absorption structure at different temperatures for F-doped $SmFeAsO_{0.931}F_{0.069}$. The inset shows an expanded energy scale view of the pre-edge structure. (b) A typical Fe *K*-edge XANES structure at different temperatures for $SmFeAsO_{0.931}F_{0.069}$ samples. The inset shows the expanded plot of absorption threshold for various temperatures. Dashed lines indicate derivatives of XANES spectra.

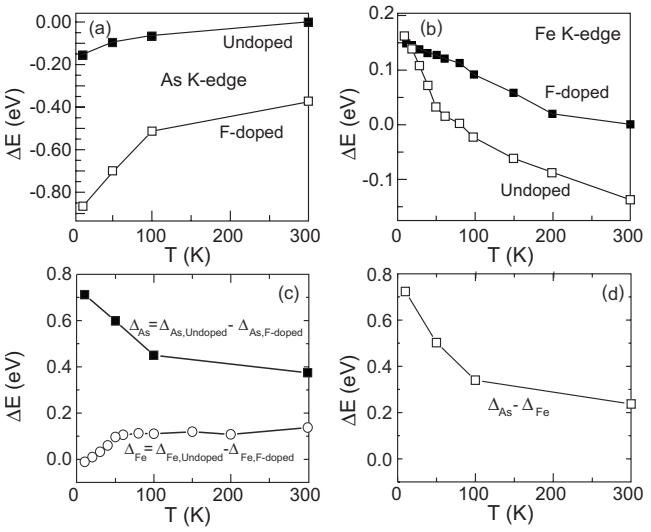

FIG. 4. The energy shift of the absorption edge as a function of temperature, for (a) As *K* edge and (b) Fe *K* edge. The energy of the absorption edge at 300 K of undoped SmFeAsO is defined as zero. (c) Energy difference of edge positions in electron volts between undoped and doped SmFeAsO samples, Δ_{As}, Δ_{Fe}. (d) Energy difference between the As and the Fe edge thresholds $\Delta_{As}-\Delta_{Fe}$ as a function of temperature.

shown in Fig. 3(a). The As *K*-edge XANES spectra showed three distinct band features, labeled A, B, and C, similar to those of $LaFeAsO_{1-x}F_x$.[12] Feature A is related to the unoccupied As(*p*)-Fe(*d*) hybridized states just above E_F. The lowest-energy part of absorption edge, assigned to excitations from the As 1*s* core level into unoccupied As 4*p* states, exhibited a systematic shift to lower energy with decreasing temperature as shown in the inset. The shift of absorption threshold toward lower energy implies a lowering of energy difference between the core level and unoccupied states with the As 4*p* character based on a dipole transition, mostly due to the lowering of unoccupied states (chemical shift). A remarkable contrast between the As *K*-edge and the Fe *K*-edge data was found in the opposing slopes (temperature coefficients) of energy shift, i.e., a positive (Fe) shift and a negative (As) shift as temperature decreased. The Fe *K*-edge XANES spectra at different temperatures for the $SmFeAsO_{0.931}F_{0.069}$ sample are shown in Fig. 3(b). The pre-edge region between 7.1066 and 7.1103 keV is related to excitations from the Fe 1*s* core level into unoccupied Fe 3*d* states. The main absorption edge in the 7.1118–7.1191 keV region is ascribed to excitations from the Fe 1*s* core level into unoccupied Fe 4*p* states.

In order to analyze the energy shift quantitatively, the absorption edge energy was defined as the first inflection point of the threshold. The energy positions of the absorption thresholds measured from an undoped sample (at 300 K) were plotted as a function of temperature for undoped and F-doped SmFeAsO samples in Figs. 4(a) and 4(b). The magnitude of the As *K*-edge energy shift between 300 and 10 K data was about 0.15 eV and 0.50 eV for undoped and doped samples, respectively, while the Fe *K*-edge variation was about 0.14 eV and 0.30 eV for undoped and doped samples, respectively. The observed edge shift for Fe *K*-edge and As *K*-edge were opposite in sign and became significant in magnitude for the superconducting sample. Note that the edge shift rapidly increases its magnitude below about 50 K, which is close to the superconducting transition temperature.

The doping-induced edge shift toward lower energy indicates that the unoccupied density of states decreases, filled by electrons. This confirms that at room temperature, doped electrons are introduced into both the As and the Fe local states when O sites are replaced by F ions. Similar to charge transfer from the La(Sr)-O charge reservoir layer to the Cu-O conductive layer in $La_{1.85}Sr_{0.15}CuO_4$, the charge carriers (electrons) are transferred from the Sm-O(F) layer to the Fe-As layer. As illustrated by energy difference (c) between the doped and the undoped samples Δ_{As} and Δ_{Fe} and (d) between the Fe and As edge $\Delta_{As}-\Delta_{Fe}$, the electron accumulation on the As sites with decreasing temperature is implicated. A reversal of edge shift indicates a possible redistribution of charge between Fe and As atoms. The doped electron density on the As atom increased as temperature was lowered, which suggests temperature-dependent intralayer charge redistribution (band filling). Indeed, a strong temperature-dependent dispersion was found for $Ba_{0.6}K_{0.4}Fe_2As_2$, which is expected to exhibit orbital-selective mode coupling.[27] The doped electrons may be accommodated in a particular electron pocket with an As atomic-orbital character at low temperature.

IV. CONCLUSION

Temperature-dependent local lattice distortion (signature of polaron formation upon doping) was found in the Fe-As displacement in $SmFeAsO_{1-x}F_x$ (x=0.045, 0.069) superconductors. Overall features of lattice anomaly (upturn of relative displacement followed by a sharp drop associated with superconducting coherence) is similar to those reported for cuprates and $LaFeAsO_{1-x}F_x$ (x=0.07) indicating intimacy between local lattice and superconductivity in both systems. Observed lattice distortion is modeled by long and short Fe-As bonds separated by about 0.1 Å (less significant than cuprates) that would increase band splitting and remove de-

generacy of bands crossing the Fermi level. Although the calculated electron-phonon coupling constant λ is unfavorable to phonon-mediated mechanism, interband interaction in multiband multigap superconductors is strongly dependent on local distortion and may play an important role in microscopic mechanism of high-temperature superconductivity. Systematic energy shifts for the Fe *K*-edge and As *K*-edge absorption thresholds indicate a temperature-dependent redistribution of doped carriers and complex band filling. Detailed knowledge on temperature-dependent band filling would be crucial for understanding microscopic mechanism of superconductivity in oxypnictides.

ACKNOWLEDGMENTS

The authors express their thanks to A. Bussmann-Holder, H. Koizumi, and T. Kakeshita for their fruitful discussions. The EXAFS experiments were conducted under Proposal No. 2008G549 at the Photon Factory, Tsukuba, Japan. The author (C.Z.) acknowledges Grant-in-Aid for JSPS Fellows for financial support to this work.

*Author to whom correspondence should be addressed; h.oyanagi@aist.go.jp

[1] P. A. Lee, N. Nagaosa, and X.-G. Wen, Rev. Mod. Phys. **78**, 17 (2006).
[2] Y. Kamihara, T. Watanabe, M. Hirano, and H. Hosono, J. Am. Chem. Soc. **130**, 3296 (2008).
[3] H. Takahashi, K. Igawa, K. Arii, Y. Kamihara, M. Hirano, and H. Hosono, Nature (London) **453**, 376 (2008).
[4] X. H. Chen, T. Wu, G. Wu, R. H. Liu, H. Chen, and D. F. Fang, Nature (London) **453**, 761 (2008).
[5] Z.-A. Ren, G.-C. Che, X.-L. Dong, J. Yang, W. Lu, W. Yi, X.-L. Shen, Z.-C. Li, L.-L. Sun, F. Zhou, and Z.-X. Zhao, EPL **83**, 17002 (2008).
[6] K. Haule, J. H. Shim, and G. Kotliar, Phys. Rev. Lett. **100**, 226402 (2008).
[7] L. Craco, M. S. Laad, S. Leoni, and H. Rosner, Phys. Rev. B **78**, 134511 (2008).
[8] D. J. Singh and M.-H. Du, Phys. Rev. Lett. **100**, 237003 (2008).
[9] V. I. Anisimov, Dm. M. Korotin, M. A. Korotin, A. V. Kozhevnikov, J. Kuneš, A. O. Shorikov, S. L. Skornyakov, and S. V. Streltsov, J. Phys.: Condens. Matter **21**, 075602 (2009).
[10] A. Y. Liu, I. I. Mazin, and J. Kortus, Phys. Rev. Lett. **87**, 087005 (2001).
[11] T. Kroll, S. Bonhommeau, T. Kachel, H. A. Dürr, J. Werner, G. Behr, A. Koitzsch, R. Hübel, S. Leger, R. Schönfelder, A. K. Ariffin, R. Manzke, F. M. F. de Groot, J. Fink, H. Eschrig, B. Büchner, and M. Knupfer, Phys. Rev. B **78**, 220502(R) (2008).
[12] A. Ignatov, C. Zhang, M. Vannucci, M. Croft, T. Tyson, D. Kwok, Z. Qin, and S. Cheong, arXiv:0808.2134 (unpublished).
[13] Y. Kamihara, T. Nomura, M. Hirano, J. E. Kim, K. Kato, M. Takata, Y. Kobayashi, S. Kitao, S. Higashitaniguchi, Y. Yoda, M. Seto, and H. Hosono, New J. Phys. **12**, 033005 (2010).
[14] H. Oyanagi, A. Tsukada, M. Naito, N. L. Saini, M.-O. Lampert, D. Gutknecht, P. Dressler, S. Ogawa, K. Kasai, S. Mohamed, and A. Fukano, J. Synchrotron Radiat. **13**, 314 (2006).
[15] A. Bianconi, N. L. Saini, A. Lanzara, M. Missori, T. Rossetti, H. Oyanagi, H. Yamaguchi, K. Oka, and T. Ito, Phys. Rev. Lett. **76**, 3412 (1996); N. L. Saini, A. Lanzara, H. Oyanagi, H. Yamaguchi, K. Oka, T. Ito, and A. Bianconi, Phys. Rev. B **55**, 12759 (1997).
[16] M. Newville, J. Synchrotron Radiat. **8**, 322 (2001).
[17] J. J. Rehr, J. Mustre de Leon, S. I. Zabinsky, and R. C. Albers, J. Am. Chem. Soc. **113**, 5135 (1991).
[18] S. Margadonna, Y. Takabayashi, M. T. McDonald, M. Brunelli, G. Wu, R. H. Liu, X. H. Chen, and K. Prassides, Phys. Rev. B **79**, 014503 (2009).
[19] C. J. Zhang and H. Oyanagi, Phys. Rev. B **79**, 064521 (2009).
[20] C. J. Zhang, H. Oyanagi, Z. H. Sun, Y. Kamihara, and H. Hosono, Phys. Rev. B **78**, 214513 (2008).
[21] J. Zhao, Q. Huang, C. Cruz, S. Li, J. W. Lynn, Y. Chen, M. A. Green, G. F. Chen, G. Li, J. L. Luo, N. L. Wang, and P. Dai, Nature Mater. **7**, 953 (2008).
[22] J. Mustre de Leon, M. Acosta-Alejandro, S. D. Conradson, and A. R. Bishop, J. Synchrotron Radiat. **12**, 193 (2005).
[23] See supplementary material at http://link.aps.org/supplemental/10.1103/PhysRevB.81.094516 for planar local lattice distortion models and simulated nearest-neighbor EXAFS oscillations which demonstrate the existence of long and short bond lengths due to polaron formation.
[24] A. Bussmann-Holder and H. Keller, Eur. Phys. J. B **44**, 487 (2005).
[25] H. Koizumi, J. Phys. Soc. Jpn. **77**, 034712 (2008).
[26] L. Boeri, O. V. Dolgov, and A. A. Golubov, Phys. Rev. Lett. **101**, 026403 (2008).
[27] P. Richard, T. Sato, K. Nakayama, S. Souma, T. Takahashi, Y.-M. Xu, G. F. Chen, J. L. Luo, N. L. Wang, and H. Ding, Phys. Rev. Lett. **102**, 047003 (2009).